

# **Electronic Supporting Information**

## **Graphene Oxide Nanohybrids for Electron Transfer Mediated Antimicrobial Activity**

Nayan Mani Das,<sup>\*a,b</sup> Amit Kumar Singh,<sup>\*b</sup> Debdatta Ghosh,<sup>a</sup> Dipankar Bandyopadhyay<sup>\*a,b</sup>

<sup>a</sup>Department of Chemical Engineering, Indian Institute of Technology Guwahati, Assam -  
781039, India.

<sup>b</sup>Centre for Nanotechnology, Indian Institute of Technology Guwahati, Assam - 781039, India.

\*E-mail: nayanmanidas3@gmail.com, amitiitg2011@gmail.com, dipban@iitg.ernet.in

## 1. Characterization of Graphene Oxide (GO) nanosheets

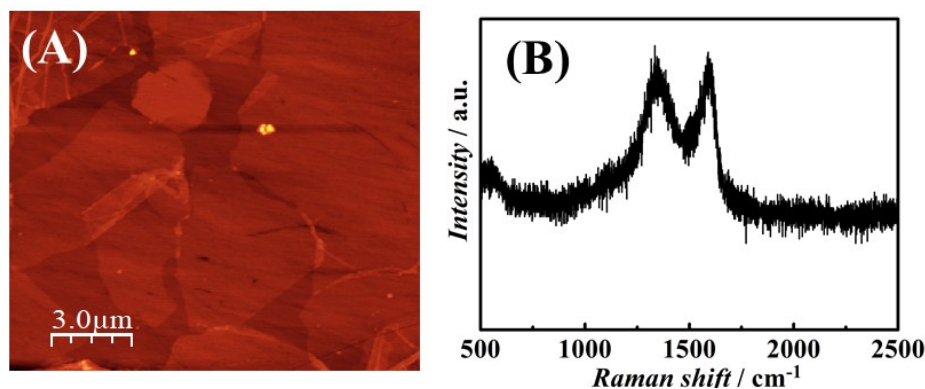


**Figure S1.** (A) Atomic force microscopy (AFM) topographic image and (B) Raman spectrum of GO nanoflakes deposited over Si surface. The scale bar in image (A) is of 3 μm.

The **Figure S1(A)** shows the AFM images of graphene oxide (GO) flakes deposited over (100) plane-orientated silicon (Si) substrate, using AFM in the tapping mode. The GO deposits had an average height of ~1.5 nm, which corresponded to presence of ~2-3 stacked GO layers.<sup>1</sup> The Raman spectrum of GO flakes<sup>2</sup> in the **Figure S1(B)** shows characteristic D band at 1350 cm<sup>-1</sup> and prominent G band at 1608 cm<sup>-1</sup>.

## 2. XPS measurements

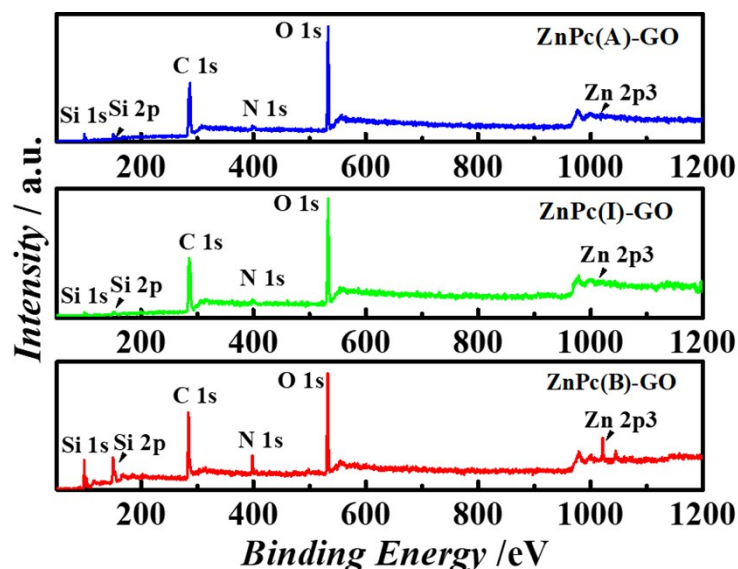


**Figure S2.** The XPS spectra of ZnPc(A)-GO, ZnPc(I)-GO and ZnPc(B)-GO nanomaterials.

The **Figure S2** shows the XPS spectra of ZnPc(A)-GO, ZnPc(I)-GO and ZnPc(B)-GO nanocomposites. The peak corresponding to the elemental silicon - Si 1s could be observed from the Si (100) substrate, whereas the elemental peaks of the Carbon (C), Nitrogen (N), Oxygen (O), and Zinc (Zn) atoms were observed from the ZnPc-GO nanocomposites. The two main

prominent peaks corresponding to the C 1s and O 1s species was observed at 286.12 eV and 531.4 eV, respectively, which mainly corresponded to GO nanosheet and two additional peaks of Zn 2p<sup>3</sup> and N 1s were observed at 1016.3 eV and 398.3 eV, respectively, from ZnPc-GO nanocomposites.<sup>3</sup>

**Table S1.** Lorentzian deconvoluted C1s XPS spectral data of nanocomposites.

Figure	Samples	Temperature	Binding Energy (B.E.) value for different bond types (in eV)				$\chi^2$ - value for curve fitting
			C=C	C-N	C-O	C=O	
5 (A)	ZnPc (A)-GO	25 °C	284.4	285.3	287.1	288.6	0.9987
5 (B)	ZnPc(I)-GO	100 °C	284.4	285.2	286.9	287.9	0.9983
5 (C)	ZnPc (B)-GO	280 °C	284.2	285.3	287.1	--	0.9988

The **Table S1** shows the peak positions of C=C, C-N, C-O and C=O interactions. The respective curve fitting parameters used for deconvolution of ZnPc(A)-GO, ZnPc(I)-GO and ZnPc(B)-GO XPS spectra for C peaks in the **Figure 5(A-C)** of the manuscript.

### 3. Surface Potential (SP) calculations

**Table S2:** Calculation of work function of the sample ( $\phi_s$ ) of the various sample.

Sample Name	Figure No.	$T_{in}$	$T_s$	$V_{CPD}$ (in V)	$\phi_t$ (in eV)	Calculated $\phi_s$ (in eV) $\phi_s = \phi_t - eV_{CPD}$
ZnPc(A)-GO	6(C)	--	--	0.014	4.52	4.504
ZnPc(I)-GO	6(D)	--	--	0.013	4.52	4.506
ZnPc(B)-GO	6(E)	--	--	0.012	4.52	4.508
ZnPc(B)-GO - <i>E. coli</i>	8(C)	0	0 min	0.082	4.52	4.438
	8(D)	0	30 min	0.061	4.52	4.459
	9(C)	2 h	0 min	0.067	4.52	4.453
	9(D)	2 h	30 min	0.032	4.52	4.488
	9(E)	2 h	1 h	0.021	4.52	4.499

The KPFM measures Contact Potential Difference ( $V_{CPD}$ ) between the AFM tip and the sample.<sup>4</sup> The surface potential of the sample ( $\phi_s$ ) is defined as:

$$\phi_s = \phi_t - eV_{CPD}, \quad (1)$$

$$\phi_s = \phi_t - V_{CPD} \text{ [where, } e = 1] \quad (2)$$

where,  $e$  = elementary charge of an electron in atomic units and its value is unity,  $V_{CPD}$  = the contact potential difference in V of sample measured by KPFM method,  $\phi_s$  = work

function of the sample in eV to be determined and,  $\phi_t$  = work function of the AFM tip in eV.

The **Table S2** shows the calculated work function of the sample ( $\phi_s$ ) of ZnPc(A)-GO, ZnPc(B)-GO and the ZnPc(B)-GO-*E. coli* samples, along with corresponding Figure numbers. In the table,  $T_{in}$  denotes the incubation time period of the samples and  $T_s$  denotes the time duration of the sample kept stand-by at the room temperature after incubation, prior to the KPFM measurements.

#### 4. FESEM images of a *E. coli*

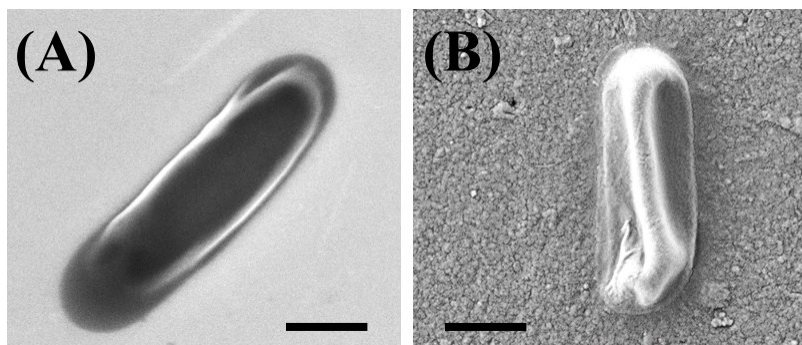


**Figure S3.** The FESEM images of a (A) healthy and (B) deformed *E. coli* cell. The scale bars in both images are of 1  $\mu\text{m}$ .

The **Figure S3(A)** demonstrates the FESEM images of a healthy *E. coli* cell and **Figure S3(B)** shows the image of an adhered *E. coli* cell on the ZnPc(B)-GO nanocomposites, captured after 2 h incubation of the ZnPc(B)-GO samples in bacterial solution. The FESEM images in **Figure S3(B)**, clearly shows the deformation in the *E. coli* bacterial cell, thereby, indicating the onset of cell membrane degradation.<sup>5</sup>

#### 5. ZnPc(B)-GO efficacy test:

We performed confocal microscopy measurements in order to interpret the efficacy of ZnPc(B)-GO. The water diluted green fluorescence protein (GFP) expressing *E. coli* bacteria solution in LB buffer media were poured over ZnPc(B)-GO substrate for 1 h and then the substrate was gently taken out of the solution. The substrate was cleaned by deionized water to remove the unadhered bacteria and then dried by passing  $\text{N}_2$  gas flow for a few seconds. The ZnPc(B)-GO substrates with GFP expressing *E. coli* were taken to the confocal microscopy for imaging. We performed the microscopy in the Zeiss (JSM-7610F) confocal instrument using the 488 nm laser as excitation wavelength and the emission was calculated in the range of 505 nm 700 nm. After imaging them at room temperature the same substrates were incubated at 37°C for about 2 h and

was again taken for the confocal microscopy. The confocal images of the GFP expressing bacteria before and after the incubation had been shown in **Figure S4**. The green fluorescence expressing *E. coli* bacteria (**Figure S4(a)**) number were seemed to gradually deemed in its fluorescence ability due to the cytoplasm leakage as shown in **Figure S4(b-d)**. The deemed in fluorescence properties of the GFP expressing *E. coli* bacteria is because of the rupture of the cell wall and for bleeding cytoplasmic materials to the surroundings.

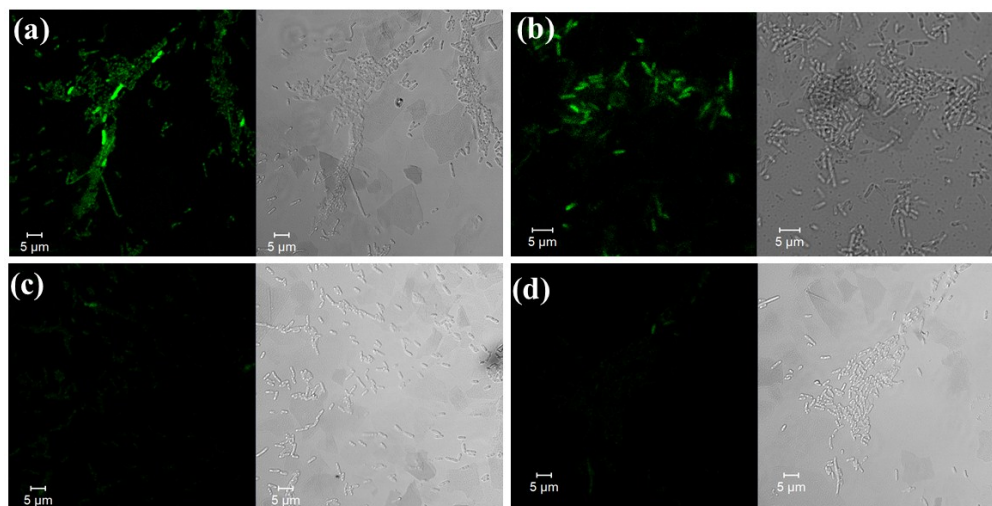


**Figure S4:** (a) Confocal microscopy image of GFP expressing *E. coli* bacteria over ZnPc(B)-GO just after deposition. Then the same sample was incubated for 2 h and the confocal microscopy images (b) 0 h after incubation (c) 30 min after incubation (d) 1 h after incubation are shown. The corresponding bright field image of the respective zone are also incorporated.

## 6. Cytoplasmic leakage test:

In order to confirm the cytoplasmic leakage as the fluorescence were found to be deemed in the GFP expressing bacteria, we carried out the UV-Visible absorption spectroscopy of the bacteria when treated with the ZnPc(B)-GO substrates. Since the extraction of the cytoplasm from dead bacteria residing over the substrates were difficult, we therefore made a solution of ZnPc(B) and GO solution in deionized water and then the *E. coli* bacteria in LB medium was added to the ZnPc(B)-GO solution and kept the solution still for about 1 h. The conditions were all kept the same as in case of the bacteria adhering to the thin films. Thereafter, the solutions were centrifuged to take out the supernatant and the UV-Visible absorption was carried out. In order to confirm the absorption peak of the cytoplasm (mainly contained the nucleic acids and proteins) we also carried out the controlled experiments where *E. coli* were treated with neutral surfactant like triton-X100 and then centrifuged to get the supernatant of the same. The absorption spectra of both the supernatant extracts of the control and the experimented solutions were compared to approve the cytoplasmic leakage. A comparative UV-Visible absorption spectroscopy has been demonstrated in the **Figure S5(a-c)**. There is a clear evidence of emergence of a combined broad

peak at wavelength around 260-280 nm. This confirmed the existence of both nucleic acid and protein as shown by the deconvolution of the absorption envelop in **Figure S5(b)** and **S5(c)**, respectively.

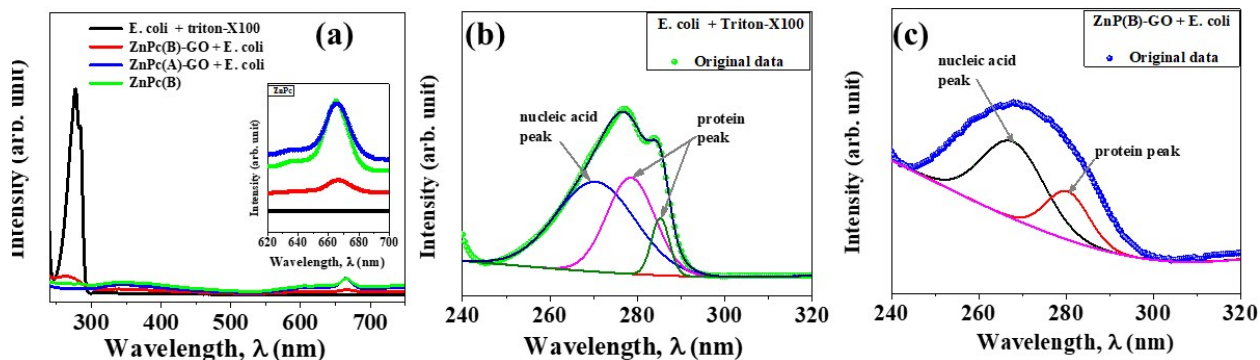


**Figure S5:** (a) The comparison of the UV-Visible absorption peaks of ZnPc(B), ZnPc(A)-GO+ *E. coli*, ZnPc(B)-GO+ *E. coli* and the controlled experiment with *E. coli* +triton-X100. In the inset the characteristic ZnPc peak is shown in enlarged way to figure out the composition. (b) The deconvolution of the absorption peak of *E. coli* while treated with triton-X100 showed solid nucleic acid and protein peaks at 269.5 nm and 278.7 and 285.2 nm respectively. (c) the deconvolution of ZnPc(B)-GO+ *E. coli* absorption peak also showed nucleic acid and protein peaks at 266.8 nm and 280.1 nm respectively.

## 7. ROS dependent oxidative stress generation:

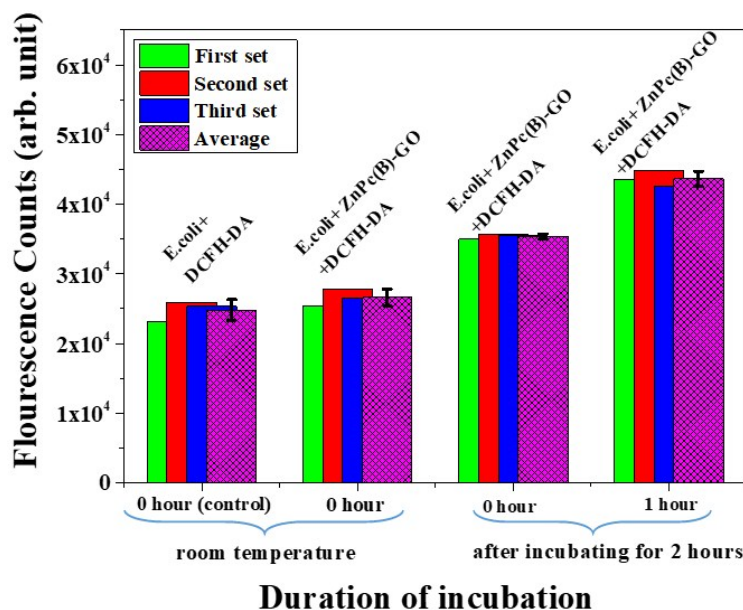


**Figure S6:** The generation of ROS levels were calculated by counting the fluorescent by using the microplate assay reader kit. Excitation wavelength of 495 nm was used and the emission were measured at 529 nm. We performed the control to be the interaction *E. coli* cells with DCFH-DA at room temperature. The preceding histograms in the figure showed the interaction of ZnPc(B)-GO with *E. coli* cells when DCFH-DA is added. The graphs were taken at room temperature and after incubation for 2 h and at 0.5 h intervals.

In order to calculate the reactive oxidative species (ROS) dependent oxidative stress generation due to interaction of ZnPc(B)-GO with *E. coli*, we measured the fluorescence by multiplate assay reader kit. We used 495 nm as the excitation wavelength and the emission was calculated at 529 nm. The fluorescent quantity was analysed by using the DCFH-DA stain where their interaction with the *E. coli* cells at room temperature was taken to be control experiment and the generation of ROS after incubation for about 2 h and a consecutive reading for another 1 h with a 30-min interval was shown in the **Figure S6**. The fluorescent analysis of the prepared ZnPc(B)-GO + *E. coli* with DCFH-DA were performed to quantify intracellular levels of ROS. We could conclude from the figure S6 that the DCFH-DA fluorescence of cells increased significantly with increased after incubation, suggesting that ZnPc(B)-GO could induce ROS accumulation in *E. coli* cells.

## 8. The $\zeta$ -potential measurements

**Table S3:** Measurement of zeta potentials ( $\zeta$ ) of the individual components in NMP solution

Samples	$\zeta$ -potential
GO (in NMP)	-7.25 mV
ZnPc (in NMP)	+3.82 mV
ZnPc-GO (in NMP)	-4.74 mV
GO (in water)	-35.44 mV

In the **Table S3**, we carried out the  $\zeta$ -potential measurements of the solutions of GO, ZnPc and ZnPc-GO in NMP (n-methyl-2-pyrrolidone). As ZnPc doesn't dissolve in pure water, we used NMP as the common solvent for both. It is reported that GO is also solvable in NMP.<sup>6</sup> For the convenience of  $\zeta$ -potential characterization, we have also included the value of GO in water too.

## REFERENCES

1. Q. Lai, S. Zhu, X. Luo, M. Zou and S. Huang, *AIP Adv.*, 2012, **2**, 2–7.
2. J. Zhu, Y. Li, Y. Chen, J. Wang, B. Zhang, J. Zhang and W. J. Blau, *Carbon*, 2011, **49**, 1900–1905.
3. Z. Wang, C. He, W. Song, Y. Gao, Z. Chen, Y. Dong, C. Zhao, Z. Li and Y. Wu, *RSC Adv.*, 2015, **5**, 94144–94154.
4. H. Huang, H. Wang, J. Zhang and D. Yan, *Appl. Phys. A Mater. Sci. Process.*, 2009, **95**, 125–130.
5. S. S. Nanda, D. K. Yi and K. Kim, *Sci. Rep.*, 2016, **6**, 28443.
6. J. I. Paredes, S. Villar-Rodil, A. Martinez-Alonso, and J. M. D. Tascon, *Langmuir* 2008, **24**, 10560-10564.